

# THERMO-MECHANICAL RESPONSE OF AN IN-SITU COPPER-BASED COMPOSITE

K.L.Lee, A.F. Whitehouse, A.C.F. Cocks

*Department of Engineering, University of Leicester  
University Road, Leicester LE1 7RH, UK*

**SUMMARY:** The mechanical response of in-situ copper-chromium composite was modelled using a deformation mechanism map approach. The stresses in each phase were predicted as a function of temperature and strain rate. From this the ratio of phase stresses, and hence the degree of load transfer, was obtained. The extent of load transfer and the predicted deformation modes of the two phases were then related to the expected failure mechanisms of the composite. Three modes of composite failure were predicted. Copper-chromium in-situ composite, and pure copper, were produced by a casting and swaging route. The mechanical properties were then characterised experimentally by tensile testing. Mechanical tests confirmed that the composite showed significantly higher strength than the unreinforced material. The observed failure modes of the composite were compared with the predictions.

**KEYWORDS:** in-situ composite, Cu-Cr, damage, failure mechanism, load transfer

## INTRODUCTION

The current demand is for conductive materials with mechanical properties which are superior to those exhibited by monolithic copper. In-situ composites provide a solution to this problem by the introduction of a stiffer reinforcement phase which bears a significant proportion of the applied load [1-5]. This allows the material to carry higher loads than unreinforced copper. At the same time, there are two obvious advantages in using in-situ composites. Firstly, conventional processing techniques, such as casting, can be employed, resulting in lower production costs compared with conventional composites, and secondly, the reinforcement phase can contribute to the conductivity, unlike traditional ceramic reinforcements [6]. It has been established that metals with bcc structure are particularly suited to reinforcing an fcc metal matrix [7], because when subjected to high degrees of deformation, they elongate preferentially, resulting in a fine ribbon-like morphology.

To date, considerable work has been directed towards the initial development of high thermal and electrical conductivity materials with high strength [8]. However, industry still faces problems in using this research for electronics and aerospace applications. The main area of focus of the currently available studies has been that of production and optimisation of the as-fabricated properties [5]. For instance, considerable work has been done on Cu-based alloys prepared by rapid solidification and mechanically alloyed metal composites [9], both to optimise the mechanical and thermal processing parameters, and to characterise the initial microstructure. In Japan, considerable research has been done on cast/drawn Cu-Cr composites which has concentrated on optimising initially the tensile strength and conductivity in terms of processing variables and subsequent ageing behaviour [10,11].

However, important questions remain unanswered. The in-service response of these materials has not been investigated. Without this knowledge they cannot be fully and safely exploited. The effect of load transfer, thermo-mechanical loading and the ensuing damage cannot be ignored. Damage will have a deleterious effect on both the conductivity of the composite, and its mechanical response. Moreover, their properties cannot be well understood without considering them in terms of composite theory; an approach which has not previously been examined.

### **Load Transfer and Misfit in Metal/Metal Composites**

In a conventional MMC, elastic and/or plastic deformation in the matrix causes a misfit between the matrix and the reinforcement, which in turn results in load transfer to the reinforcement. However, Cu-Cr in-situ composites differ fundamentally from conventional composites in that both phases are able to deform plastically. Therefore, the degree of load transfer is governed by the relative extent of deformation in each phase, and this in turn depends upon the dominant deformation mechanism operating in each phase at a given temperature. In order for the composite's deformation and subsequent failure mechanisms to be fully understood, it is necessary to quantify the extent of load transfer as a function of temperature and strain rate.

In this work, the deformation rate of each phase is predicted using model-based strain-rate equations as outlined by Frost and Ashby [12]. From this the overall composite deformation rate is derived and is presented in a deformation map form. This is used to obtain information regarding the extent of load transfer in the composite as a function of testing temperature and strain rate, and hence regimes of failure mechanism. Predictions are then compared with experimental results.

## **EXPERIMENTAL PROCEDURE**

A model Cu-30 vol.% Cr in-situ composite system was selected and cast at 1600°C. The material was subsequently forged and swaged into 3 mm diameter rod, with approximately 98% reduction in area. The resulting as-processed microstructure is shown in Fig. 1 and consists of elongated ribbons of Cr in a Cu matrix..



Fig. 1: Electron micrograph showing as-processed Cu-30 vol.% Cr composite.

The composite was tested in tension at room temperature, 220°C and 410°C under displacement control at a rate of 1 mm min<sup>-1</sup>, with the Cr ribbons parallel to the loading direction. Axial and transverse strains were monitored using a video extensometer. Similar tests were also carried out on the unreinforced swaged copper. After testing, specimens were sectioned and the microstructure examined using optical and SEM techniques. Initially, specimens were mechanically polished and etched with dilute chromic acid to reveal the Cu grain structure. After this, the specimens were deep etched using 40% HNO<sub>3</sub>, prior to examination in the SEM, in order to reveal microstructural damage.

## RESULTS AND DISCUSSION

### Composite Mechanical Behaviour

Fig. 2 shows some typical tensile data for the composite and unreinforced copper. As expected, the addition of the Cr ribbons results in a significant increase in the Young's modulus and load bearing capacity of the material, with a corresponding loss in ductility. The composite failure mechanisms are discussed in the following section.

### Predictions of Composite Response

In order to quantify the extent of load transfer occurring in the composite, an Ashby deformation mechanism map approach was used [13]. Data for the deformation of Cu and Cr was taken from Frost and Ashby [12]. In this method, the strain rate due to various microstructural deformation processes, (for example diffusional creep, obstacle controlled glide etc.) is calculated for different values of applied stress and temperature. From this, the overall strain rate and the dominant mechanism operating under particular conditions can be identified. The strain rate equations used are given in the Appendix.

Initially, deformation maps were derived for the Cu and Cr phases under uniaxial applied stress. From these, the overall composite deformation rate was obtained using a standard rule of mixtures. This approach is appropriate for determining the overall deformation response of the class of composite microstructures shown in Fig. 1. A plot showing the  $\sigma_{Cr}:\sigma_{Cu}$  stress

ratio was then obtained using the calculated phase stresses. This gave a measure of the extent to which load is transferred to the reinforcement as a function of strain rate and temperature.

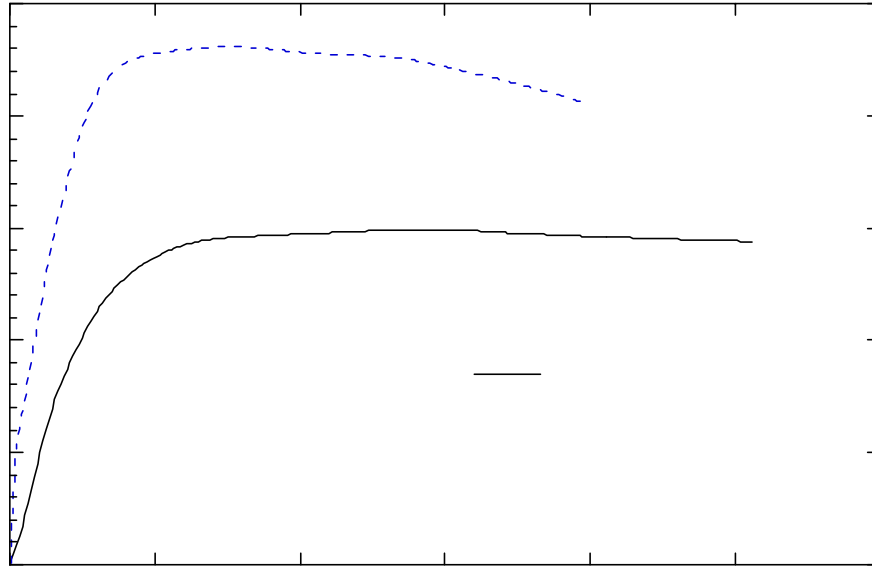


Fig. 2: Stress/strain response for unreinforced copper and copper 30 vol.% chromium in-situ composite tested at room temperature.

The deformation mechanism map for Cu-30 vol.% Cr is shown in Fig. 3. On comparison with deformation maps of the individual phases, it is found that the response is dominated by the deformation of the copper, although the increasing intrinsic lattice resistance of the Cr at low temperatures is responsible for a greater temperature sensitivity. The composite behaviour can be divided into five regimes, according to the mechanisms of deformation which dominate within each phase (as defined in Fig. 3). The overall trends are described as follows: at low temperatures, the Cr is brittle in a plastic Cu matrix, hence the two dominating mechanisms are lattice resistance controlled glide in the Cr and obstacle controlled glide in the Cu; as the temperature is increased, so both phases are able to deform plastically, and obstacle controlled glide dominates the behaviour in both Cu and Cr; at higher temperatures creep becomes the dominant deformation mechanism, first for the Cu and then for the Cr.

The material response will depend critically on the efficiency with which load is transferred to the reinforcement during deformation. This, in turn, depends on the misfit generated between the two phases. The composite deformation mechanism map (Fig. 3) confirms that the ease with which each phase deforms, and hence the degree of misfit and load transfer, is highly sensitive to both the temperature and the strain rate. This is expected to have significant consequences on the mechanical performance and failure mechanisms.

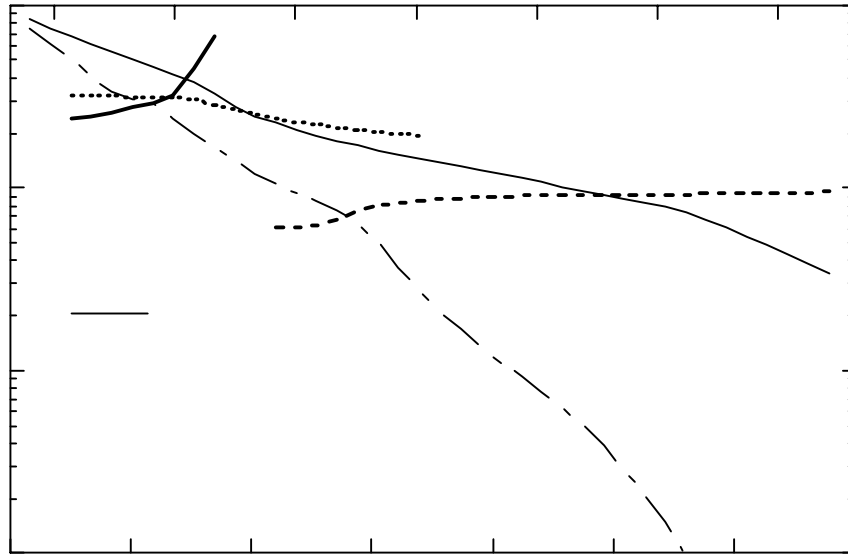


Fig. 3: Deformation mechanism map for Cu-30 vol.% Cr. The regimes I to V indicate the conditions under which certain deformation processes dominate in each of the two phases.

The ratio of Cr stress to Cu stress as a function of strain rate and temperature is presented in Fig. 4. It can be seen that the behaviour of the composite, in terms of degree of load transfer, falls into three regimes. Around room temperature, the ratio of stress in the Cr to that in the Cu is approximately one. Therefore, at this temperature both phases are deforming by similar extents, and consequently no misfit is generated between the two phases. This means that the composite behaviour is essentially that of a two-phase alloy, with no appreciable load transfer occurring. At low temperatures, the lattice resistance of the bcc Cr increases sharply, and therefore the Cr begins to behave more like the rigid reinforcement in a conventional composite. The Cu can still deform plastically, and therefore significant misfit is generated during deformation giving rise to effective loading of the Cr reinforcement phase. At elevated temperatures, creep processes become significant in the Cu, leading to much easier deformation in this phase. As a result of this, significant misfit is generated between the two phases during deformation, and the Cr reinforcement is loaded preferentially. This shows that the Cr is effective as a reinforcement only when its deformation behaviour differs significantly from that of the Cu.

It can also be seen from Fig. 4 that the deformation rate has a significant influence on the composite behaviour. As the strain rate decreases, so the response curve shifts to lower temperatures. This is to be expected, since time dependent deformation mechanisms will be more significant at lower strain rates. Therefore, under a low strain rate there will be an

increased degree of misfit, and hence more load transfer, compared with that at higher loading rates for the same temperature.

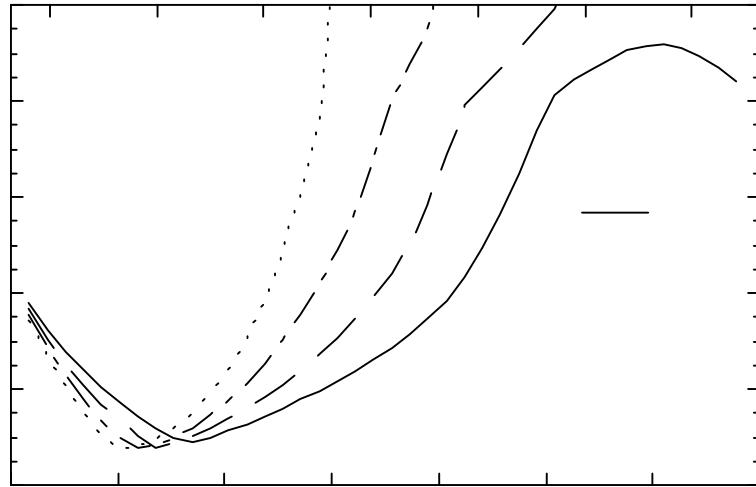


Fig. 4: Ratio of stress in the Cr and Cu phases, as a function of temperature at different strain rates. Note that around room temperature, the ratio is  $\sim 1$ , which implies that load transfer is negligible under these conditions.

Fig. 5 shows the dominant deformation mechanism regimes, as defined in Fig. 3, superimposed on the stress ratio plot. Care needs to be exercised in the interpretation of this plot. The solid line and dashed line adjoining regions IV and V represent boundaries between different classes of behaviour in the conventional sense and were determined by selecting the fastest of a number of competing mechanisms in each phase. The lower dashed boundary was determined, however, by selecting the slowest glide controlled plasticity mechanism. A consequence of this is that the constant strain rate contours do not cross this boundary. As the temperature is increased from 0 K, the stress ratio gradually decreases until the constant strain rate contour touches the lower dashed line of Fig. 5. Up to this point plastic deformation in the Cr is lattice resistance controlled. As the temperature is increased still further, obstacle controlled glide becomes the dominant mechanism in the Cr and the stress ratio increases again. Thus the minima in the stress ratio curves correspond to a change in dominant mechanism from lattice resistance controlled glide to obstacle controlled glide within the Cr phase.

These observations on load transfer have important implications for the expected failure mechanisms of the composite. At low temperatures, load transfer occurs to the Cr, and, since it is brittle because of its high lattice resistance, damage is expected to occur in the form of reinforcement cracking. This has been observed experimentally [14]. At intermediate temperatures, where there is no significant load transfer, a simple ductile failure should be observed, without any of the damage typically observed in conventional MMCs. At high temperatures, load transfer will result in significant stresses within the Cr reinforcement. However, unlike the low temperature situation, the Cr is ductile and unlikely to fracture. Damage is therefore expected to occur at the interface between the two phases, in the form of cavitation [15], particularly at the tips of the reinforcement, where the local stresses will be higher than those calculated here. Although extensive experimental results are not yet

available, preliminary findings agree well with the predicted behaviour. The tensile tests performed corresponded to a strain rate of  $\sim 10^{-3}\text{s}^{-1}$ . The model predicts stress ratios of 1.06 at 20 °C and 2.6 at 410°C for this strain rate. This would suggest that microstructural damage due to local stresses would not be expected during the room temperature tests, but would be increasingly likely as the test temperature is increased. Fig. 6 shows micrographs taken from specimens of Cu 30 vol.% Cr tested at 20°C and 410°C, remote from the fracture surface. It can be seen that damage in the form of cavitation only occurs at the higher temperature, which agrees well with the predicted load transfer temperature dependency. There is no significant microstructural damage in the specimen tested at room temperature.

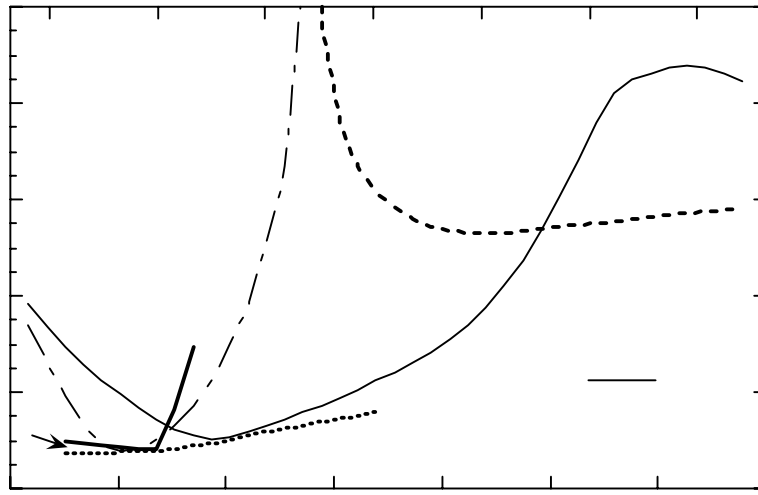


Fig. 5: Stress ratio plot showing regimes of dominant deformation mechanism.

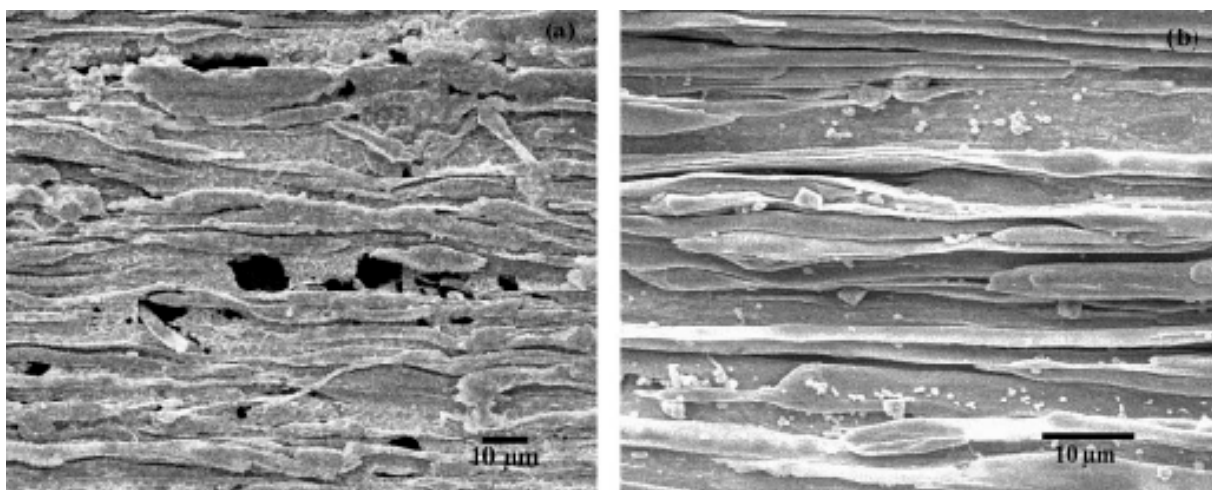


Fig. 6: Specimens of failed Cu 30 vol.% Cr tested at (a) 410°C and (b) 20°C viewed using SEM. Note that cavitation occurs at high temperatures, but not at room temperature.

## CONCLUSIONS

- The concepts of load transfer and misfit between phases have been applied to an in-situ Cu-Cr composite to explain the observed mechanical response and failure mechanisms.
- A deformation mechanism approach has been used to give information regarding the overall composite deformation rate, and the extent of load transfer within metal/metal composites under different temperature and strain rate conditions. Regimes of dominant deformation mechanism have been identified.
- Around room temperature the degree of misfit, and hence load transfer to the Cr, during deformation is insignificant. At low temperatures the Cr becomes brittle, leading to behaviour akin to that of conventional composites where the load is transferred to the reinforcement. Significant creep in the Cu at high temperatures results in appreciable misfit and load transfer.
- Significant load transfer results in high local stresses which initiate damage processes, such as reinforcement fracture or cavitation. Preliminary experimental findings agree well with these predictions.

## ACKNOWLEDGEMENTS

The authors wish to acknowledge the financial support of the EPSRC. Thanks are also due to Mr. K. Roberts of Cambridge University Materials Science Department, Dr. S. Sun, Miss H. Carroll, Mr. C. Morrison and Mr. A. Lightfoot of Leicester University. Professor I. Postlethwaite is thanked for the provision of laboratory facilities.

## REFERENCES

1. Spitzig, W.A., Downing, H.L., Laabs, F.C., Gibson, E.D. and Verhoeven, J.D., *Strength and Electrical-Conductivity Of a Deformation-Processed Cu-5 Pct Nb Composite*, Metallurgical Transactions a-Physical Metallurgy and Materials Science, Vol. 24(1), 1993, pp. 7-14.
2. Biselli, C. and Morris, D.G., *Microstructure and Strength Of Cu-Fe In-Situ Composites After Very High Drawing Strains*, Acta Materialia, Vol. 44(2), 1996, pp. 493-504.
3. Liu, P., Bahadur, S. and Verhoeven, J.D., *The Mechanical and Tribological Behavior Of Cu-Nb In-Situ Composites*, Wear, Vol. 166(2), 1993, pp. 133-139.
4. Kim, S.T., Berge, P.M. and Verhoeven, J.D., *Deformation-Processed Copper-Chromium Alloys - Optimizing Strength and Conductivity*, Journal Of Materials Engineering and Performance, Vol. 4(5), 1995, pp. 573-580.
5. Verhoeven, J.D., Spitzig, W.A., Schmidt, F.A., Krotz, P.D. and Gibson, E.D., *Processing to Optimize the Strength Of Heavily Drawn Cu-Nb Alloys*, Journal Of Materials Science, Vol. 24(3), 1989, pp. 1015-1020.
6. Whitehouse, A.F. and Clyne, T.W., *Electrical Resistivity of Copper Reinforced with Short Carbon Fibres*, J. Mat. Sci., Vol. 26, 1991, pp. 6176-6182.

7. Verhoeven, J.D., Spitzig, W.A., Jones, L.L., Downing, H.L., Trybus, C.L., Gibson, E.D., Chumbley, L.S., Fritzscheier, L.G. and Schnittgrund, G.D., *Development Of Deformation Processed Copper Refractory-Metal Composite Alloys*, Journal Of Materials Engineering, Vol. 12(2), 1990, pp. 127-139.
8. Ellis, T.W., Kim, S.T. and Verhoeven, J.D., *Deformation-Processed Copper-Chromium Alloys - Role Of Age-Hardening*, Journal Of Materials Engineering and Performance, Vol. 4(5), 1995, pp. 581-586.
9. Biselli, C. and Morris, D.G., *The High-Temperature Deformation Of Mechanically Alloyed Copper-Based Alloys*, Materials Science and Engineering a-Structural Materials Properties Microstructure and Processing, Vol. 148(2), 1991, pp. 163-173.
10. Jin, Y., Adachi, K., Takeuchi, T. and Suzuki, H.G., *Microstructural evolution of a heavily cold-rolled Cu-Cr in situ metal matrix composite*, Materials Science and Engineering a-Structural Materials Properties Microstructure and Processing, Vol. 212(1), 1996, pp. 149-156.
11. Jin, Y., Adachi, K., Takeuchi, T. and Suzuki, H.G., *Correlation between the cold-working and aging treatments in a Cu-15 wt pct Cr in situ composite*, Metallurgical and Materials Transactions a-Physical Metallurgy and Materials Science, Vol. 29(8), 1998, pp. 2195-2203.
12. Frost, H.J. and Ashby, M.F., *Deformation Mechanism Maps - The Plasticity and Creep of Metals and Ceramics*, 1, Pergamon, Oxford, 1982, pp. 161.
13. Ashby, M.F., *The First Report on Deformation Mechanism Maps*, Acta Metall., Vol. 20, 1972, pp. 887.
14. Whitehouse, A.F. *Optimisation of Mechanical and Electrical Properties of Copper-Chromium Composite.*, Report, (1996), National Research Institute for Metals, Japan.
15. Whitehouse, A.F. and Clyne, T.W., *Critical Stress Criteria For Interfacial Cavitation In MMCs*, Acta Metallurgica Et Materialia, Vol. 43(5), 1995, pp. 2107-2114.

## APPENDIX

The following equations were utilised in order to obtain the composite deformation mechanism maps. Notation is consistent with that of Frost and Ashby [12].

The strain rate due to discrete obstacle controlled plasticity in each phase,  $\dot{\epsilon}_2$ , is given by:

$$\dot{\epsilon}_2(\sigma, T) = \frac{\gamma_0}{\sqrt{3}} \exp\left[\frac{-\Delta F}{kT} \left(1 - \frac{\sigma}{\sqrt{3}\tau}\right)\right] \quad (1)$$

where  $\tau$  is the obstacle controlled glide flow stress at 0 K,  $\gamma_0$  is the pre-exponential and  $\Delta F$  the activation energy for obstacle controlled glide and  $k$  is the Boltzman constant.

The strain rate due to lattice resistance limited plasticity in Cr,  $\dot{\epsilon}_3$ , is given by:

$$\dot{\epsilon}_3(\sigma, T) = \frac{\gamma_p}{\sqrt{3}} \left( \frac{\sigma}{\sqrt{3}\mu(T)} \right)^2 \exp \left[ \frac{-\Delta F_p}{kT} \left[ 1 - \left( \frac{\sigma}{\sqrt{3}\tau_p} \right)^{3/4} \right]^{4/3} \right] \quad (2)$$

where  $\tau_p$  is the lattice resistance controlled glide flow stress at 0 K,  $\gamma_p$  is the pre-exponential and  $\Delta F_p$  the activation energy for lattice resistance controlled, and  $\mu$  is the shear modulus.

The strain rate due to power-law creep,  $\dot{\epsilon}_4$ , in Cr is given by:

$$\dot{\epsilon}_4(\sigma, T) = A \left[ D_{ov} \exp\left(\frac{-Q_v}{RT}\right) + \left(\frac{10a_c D_{oc}}{b^2}\right) \left(\frac{\sigma}{\sqrt{3}\mu(T)}\right)^2 \exp\left(\frac{-Q_c}{RT}\right) \right] \mu(T) \frac{b}{kT} \left(\frac{\sigma}{\mu(T)}\right)^n \quad (3)$$

where  $b$  is the Burger's vector,  $D_{ov}$  is the pre-exponential and  $Q_v$  the activation energy for lattice diffusion,  $R$  is the gas constant,  $a_c$  the dislocation core cross section,  $D_{oc}$  is the pre-exponential and  $Q_{oc}$  the activation energy for dislocation core diffusion,  $n$  is the power-law creep exponent and  $A$  the Dorn constant for power-law creep

The strain rate due to power-law creep and power-law breakdown,  $\dot{\epsilon}_6$ , in Cu is given by:

$$\dot{\epsilon}_6(\sigma, T) = \frac{A}{\alpha_p^n} \left[ D_{ov} \exp\left(\frac{-Q_v}{RT}\right) + 10 \left(\frac{a_c D_{oc}}{b^2}\right) \left(\frac{\sigma}{\sqrt{3}\mu(T)}\right)^2 \exp\left(\frac{-Q_c}{RT}\right) \right] \mu(T) \frac{b}{kT} \sinh\left(\frac{\sigma \alpha_p}{\mu(T)}\right)^n \quad (4)$$

where  $\alpha_p$  is the reciprocal of the normalised stress at which power-law breakdown occurs.

The strain rate due to diffusional flow in each phase,  $\dot{\epsilon}_7$ , is given by:

$$\dot{\epsilon}_7(\sigma, T) = \frac{14\sigma\Omega}{kTd^2} \left[ D_{vo} \exp\left(\frac{-Q_v}{RT}\right) + \frac{\pi}{d} \left( \delta D_{ob} \exp\left(\frac{-Q_b}{RT}\right) \right) \right] \quad (5)$$

where  $\Omega$  is the atomic volume,  $d$  is the grain size,  $\delta D_{ob}$  the boundary diffusion pre-exponential and  $Q_b$  is the boundary diffusion activation energy.

The shear modulus for each phase is given by:

$$\mu(T) = \mu_o \left( 1 + \frac{T - 300}{T_m} \cdot dT \right) \quad (6)$$

where  $\mu_o$  is the modulus at 300K,  $T_m$  is the melting point and  $dT$  is the modulus temperature dependence.